RSC Advances

ROYAL SOCIETY OF CHEMISTRY

www.rsc.org/advances

Carrier-tunable magnetism in two dimensional graphene-like C_2N

Zhaohuan Liang[1], Bo Xu[1, *], Hui Xiang[1], Yidong Xia[1], Jiang Yin[1, 2*], Zhiguo Liu[1,2]

[1]*National Laboratory of Solid State Microstructures and Department of Materials Science and Engineering, Nanjing University, Nanjing, 210093, China*

[2]*Collaborative Innovation Center of Advanced Microstructures, Nanjing University, Nanjing, 210093, China*

[*]Correspondence to: xubonju@gmail.com and jyin@nju.edu.cn.

We explore the carrier doping effect on magnetic properties in two dimensional (2D) graphene-like C_2N (g-C_2N) by performing spin-polarized density functional theory calculations. 2D g-C_2N can be induced to ferromagnetism by hole doping with a quite low critical concentration of $5\times10^{13}cm^{-2}$. Upon increasing hole density, both the magnetic moment and the magnetic coupling can be enhanced. The predicted magnetism originates from the flat bands from the non-bonding σ-states localized at the nitrogen atoms. Our findings open an opportunity to explore magnetic phenomena in 2D, and to control spin transport in 2D semiconductors by electrostatic gating.

Atomically thin two-dimensional (2D) crystals has garnered interest from researchers in various fields, due to many promising applications such as nanoelectronics[1], spintronics[2], hydrogen storage[3], batteries[4] and sensors[5]. Among these applications, controlling magnetism in 2D crystals in particular has been a persisting goal in this area, because spintronics uses the electron spin in addition to the charge for information storage, transportation and processing, and it is igniting a revolution in information processing.[6]

To fabricate spintronic device at 2D, it is one key issue to develop 2D magnets. Theoretically, numbers of 2D magnets have been proposed[7-21]. Since the discovery of graphene, many efforts have been devoted to develop 2D crystal based spintronics. By introducing adatoms[22], defects[23-25], or edges to graphene[1], ferromagnetic (FM) properties can be possibly realized even above room temperature. However, until now the experimental validation of magnetism in these systems has been scarce partly due to the low yield, small domains and rich boundaries/defects of prepared samples. Alternatively, other 2D inorganic nanosheets such as BN[10], ZnO[26], SiC[13] and transition metal dichalcogenides[26], have attracted new attention very recently for their novel electronic and magnetic properties, as well as great potential in electronic and spintronic devices. Ma *et al* studied the magnetic properties of half-fluorinated of BN, GaN and graphene[10], and proposed that magnetic coupling in these materials can be controlled by extent strain. Graphitic carbon nitride was found to exhibits a ferromagnetic ground state and intrinsic half-metallicity[8, 11]. And several investigations have been put forward to realize magnetism by introducing transition metal into 2D crystals[27-28], but no experimental evidence of formation of magnetic orders has been reported in this way so far. The possible reasons would be that all the theoretically predicted magnetic in these 2D compounds needs either the carefully selective doping or a strong external field, such as electric field and strain, which may make the experimental synthesis largely inaccessible.

Recently, a new micrometre-sized two-dimensional (2D) N-containing holey crystals: C_2N, was synthesized via a simple wet-logical reaction as a bottom-up

approach without template assistance by Mahmood *et al*.[29] In the graphene-like C_2N (*g*-C_2N), the benzene rings are bridged by pyrazine rings, which consist of a six-membered *D2h* ring with two nitrogen atoms facing each other. They found that the electronic structure of *g*-C_2N is completely different from those of graphene and h-BN, for the flat bands near the Fermi levels which originated from the localized *p* orbital of the nitrogen atoms. The flat bands near Fermi level would result in a large density of states (DOS) near Fermi level. In general, a large DOS at the Fermi level of a system, would lead to instabilities and transitions to different phases such as magnetism, superconductivity, and other phenomena. Mahmood *et al*.[29] proposed that *g*-C_2N could be ferromagnetic by hole doping. Here, we present a systematic investigation on the ferromagnetic phase transition induced by hole doping in *g*-C_2N through first-principles theoretical calculations. Our results show that both magnetic moments and magnetic coupling in *g*-C_2N can be effectively tuned by carrier doping.

Our spin-polarized DFT calculations are performed by using the Vienna ab-initio simulation package (VASP)[30-32] and adopting a Perdew-Burke-Ernzerhof (PBE)[33] gradient corrected functional for exchange and correlation potentials. The interaction between ions and electrons is described using the frozen-core projector augmented wave approach. The plane-wave kinetic energy cutoff is 450 eV. A supercell with a vacuum space of 15 Å along the *z*-direction is employed with a k-point mesh of 13 × 13 × 1. Both the lattice constant and the positions of all atoms are relaxed until the force is less than 0.01 eV/Å. The criterion for the total energy is set as 1×10^{-6} eV. Carrier doping is simulated by removing or adding electrons from the system and using a homogeneous background charge to maintain charge neutrality.

Fig. 1 presents the optimized structure of *g*-C_2N, which is composed of two benzene rings are bridged by pyrazine rings, which consist of a six-membered D2h ring with two nitrogen atoms facing each other. The optimized lattice parameter for 2D *g*-C_2N is a = b = 8.354 Å (which is also the distance between two pores), and agrees well with the experimental value (8.3 Å)[29]. Two different types of carbon

bonds are present in benzene rings: 1.428 and 1.467 Å, as displayed in Fig. 1. The C-N bond length is 1.336 Å. The angle of C-N-C is 117.4º, slightly deviated from 120º.

Fig. 2a illustrates the band structure of 2D *g*-C_2N and indicates that it is a semiconductor with band gap of 1.74 eV. It is in good agreement with previous theoretical results (1.70 eV), but smaller than the experimental results (1.96 eV)[29] determined by optical absorbance method. The PBE calculations usually underestimate the band gap of semiconductors which contain nitrogen/carbon structures[30, 31]. Both the valence band maximum (VBM) and conduction band minimum (CBM) are located at the Γ point. We also plot the density of states (DOS) and partial DOS (PDOS) of *g*-C_2N in Fig. 2b. We find that the CBM is mainly composed of p_z orbitals of the nitrogen and carbon atoms, while VBM is predominantly contributed by the non-bonding σ-states (p_x and p_y orbitals) localized of the nitrogen atoms. Interesting thing is that there is a large DOS at the top of valence band, below the Fermi level. Although intrinsic 2D *g*-C_2N is nonmagnetic, a large DOS at the Fermi level of a system, would lead to instabilities and transitions to different phases such as magnetism, superconductivity, and other phenomena. Previous works have shown that carrier doping can open a big band gap in bilayer graphene that is realized with voltage gate[36]. A carrier-doping induced antiferromagnetic to ferromagnetic transition is also theoretically predicted in 2D $MnPSe_3$ crystal[12]. Next, carrier doping is considered to manipulate the magnetic properties in 2D *g*-C_2N.

To explore the carrier doping effects on the magnetism of 2D *g*-C_2N, we calculate the magnetic moments as a function of carrier doping concentration and present the calculated results in Fig. 3a. Our calculations show that it spontaneously develops a ferromagnetic ground state even at a small amount of hole doping. We also checked the electron doping effect, there is no magnetic transition with the electron doping concentration up to 10^{15} cm^{-2}. With a small amount of hole doping (< 3.3×10^{13} cm^{-2} (0.2 hole per unit cell)), the 2D g-C_2N remains the nonmagnetic state. 2D

g-C_2N attains net magnetic moment and the FM state becomes the ground state, which can be further enhanced by increasing concentration of the doped carriers. We find an total magnetic moments of 0.167 μ_B at the hole concentration of 5×10^{13} cm^{-2} (0.3 hole per unit cell). Larger magnetic moment develops upon increasing carrier density. At the hole concentration of $8\times10^{13}cm^{-2}$ (0.5 hole per unit cell), the total magnetic moment is nearly 0.38 μ_B. Each nitrogen atom contributes 0.047μ_B, while each carbon atom only contributes 0.008μ_B. After this density, the total magnetic moment is linearly increased upon the hole density, and the magnetic moment per hole saturates at nearly 0.76μ_B/carrier, as displayed in Fig. 3. 2D *g*-C_2N can keep the ferromagnetic ground state even with the hole density up to 5×10^{14} cm^{-2}.

We also examine the energy of magnetization as a function of carrier doping concentration and present the calculated results in Fig. 3b. We check the several antiferromagnetic configurations, and we find that the antiferromagnetic states converge to nonmagnetic state at last. As we see, after the hole doping concentration is larger than 3.3×10^{13} cm^{-2}, the ferromagnetic state becomes the ground state. At the hole concentration of $1.65\times10^{14}cm^{-2}$ (1 hole per unit cell), the ferromagnetic states for one unit cell is about 22.7 meV lower than in energy than that of antiferromagnetic state.

To further understand the physical origin of ferromagnetism, a detailed analysis of the band structure and DOS of hole doped 2D *g*-C_2N has been carried out at the doping concentration of 1.6×10^{14} cm^{-2} (1 hole per unit cell) for example. We first calculated the band structure of 2D *g*-C_2N at the doping concentration of 1.6×10^{14} cm^{-2} (1 hole per unit cell) without spin polarization in Fig. 4. As we see, once extra hole is doped, the localized σ-states of nitrogen come to the Fermi level. The localized partially occupied band shows a spin splitting once the Stoner criterion[37] is met, and 2D *g*-C_2N would be magnetic. Such a transition from a nonmagnetic to a magnetic ground state is driven by the Stoner criterion, which reads $I \bullet N(E_F) > 1$, where I is the Stoner parameter (the exchange constant) and $N(E_F)$ is the DOS at the Fermi level.[38, 39] The Stoner parameter can be estimated from our DFT calculations,

since the magnetic exchange splitting, Δ, of the bands is given by Im,[40] where m is the magnetic moment in units of the Bohr magneton, μ_B. For instance, in the case of the hole concentration at 1.6×10^{14} cm^{-2} we find that Δ = 0.2 eV and m = 0.76μ_B /unit cell, so that the estimated value of the Stoner I parameter is ~0.26 eV and the required DOS at the Fermi level necessary to satisfy the Stoner instability condition is $N(E_F) \geq 1/0.26 \sim 4$ eV^{-1}. The peak of the DOS in 2D g-C_2N can reach 25 eV^{-1} as shown in Fig. 4, large enough to be ferromagnetic.

Fig. 5a and 5b present the spin polarized band structures and DOS of hole doped 2D g-C_2N, respectively. Both spin channels are metallic. Clearly, the ferromagnetism and magnetic moment are mainly attributed to the p_x and p_y orbitals of N atoms. We can confirm it in the spatial distribution of spin-polarized electron density of 2D g-C_2N (Fig. 5c). We find that the top of the valence band becomes to dispersion band, after one hole is dope in 2D g-C_2N. Combined with DOS, it is composed of p_z of carbon, which provides extended tails of wave functions for overlapping among each other and accounts for the ferromagnetic coupling between local spins. So, the magnetism is originated from the localized σ-states of nitrogen atoms, stabilized by the π-states in the benzene ring. The π-states in the benzene ring do not account for the ferromagnetic coupling, but influence the strength of the magnetic coupling. So the ferromagnetic interaction mediated by carrier concentration could be explained in terms of the RKKY model[41].

In conclusion, we investigate the hole doping effects on the magnetic properties of the 2D g-C_2N based on the spin-polarized DFT calculations. We find that hole doping induces tunable ferromagnetic properties in 2D g-C_2N. These carrier-tunable magnetism is tightly correlated with the localized σ-states of nitrogen atom. The magnetism could be realized by the gate voltage method, for the critical hole concentration is quite low, about 5×10^{13} cm^{-2}. These discovered hole doping effects on the magnetism of 2D g-C_2N provide fundamental insight of magnetism in 2D semiconductors, implying that 2D g-C_2N serves as a potential spintronic material with electric field controlled magnetism.

Acknowledgements

This work was supported by the Fundamental Research Funds for the Central Universities, a Project Funded by the Priority Academic Program Development of Jiangsu Higher Education Institutions (PAPD). We are grateful for the support of NSFC (11204123). The calculations were performed on parallel computers at the High Performance Computing Center (HPCC) of Nanjing University.

References

1. Y.-W. Son, M. L. Cohen and S. G. Louie, *Nature,* 2006, **444**, 347.
2. O. V. Yazyev, *Phys. Rev. Lett.,* 2008, **101**, 037203.
3. K. S. Novoselov, D. Jiang, F. Schedin, T. J. Booth, V. V. Khotkevich, S. V. Morozov and A. K. Geim, *Proc. Natl Acad. Sci., USA* 2005, **102**, 10451.
4. T. Takamura, K. Endo, L. J. Fu, Y. P. Wu, K. J. Lee and T. Matsumoto, *Electrochim. Acta,* 2007, **53**, 1055.
5. F. Schedin, A. K. Geim, S. V. Morozov, E. W. Hill, P. Blake, M. I. Katsnelson and K. S. Novoselov, *Nat. Mater.,* 2007, **6**, 652.
6. A. Fert, *Rev. Mod. Phys.,* 2008, **80**, 1517.
7. J. Zhou and Q. Sun, *J. Am. Chem. Soc.,* 2011, **133**, 15113.
8. A. Du, S. Sanvito and S. C. Smith, *Phys. Rev. Lett.,* 2012, **108**, 197207.
9. E. Kan, W. Hu, C. Xiao, R. Lu, K. Deng, J. Yang and H. Su, *J. Am. Chem. Soc.,* 2012, **134**, 5718.
10. Y. D. Ma, Y. Dai, M. Guo, C. W. Niu, L. Yu and B. B. Huang, *Nanoscale,* 2011, **3**, 2301.
11. X. M. Zhang, M. W. Zhao, A. Z. Wang, X. P. Wang and A. J. Du, *J. Mater. Chem. C,* 2013, **1**, 6265.
12. X. X. Li, X. J. Wu and J. L. Yang, *J. Am. Chem. Soc.,* 2014, **136**, 11065.

13. B. Xu, J. Yin, X. G. Wan, Y. D. Xia, J. Yin and Z. G. Liu, *Appl. Phys. Lett.,* 2010, **96**, 143111.

14. Y. F. Li, Z. Zhou, P. W. Shen and Z. F. Chen, *ACS Nano,* 2009, **3**, 1952.

15. J. Zhou, Q. Wang, Q. Sun, X. S. Chen, Y. Kawazoe and P. Jena, *Nano Lett.,* 2009, **9**, 3867.

16. W. Chen, Y. Li, G. Yu, C.-Z. Li, S. B. Zhang, Z. Zhou and Z. Chen, *J. Am. Chem. Soc.,* 2010, **132**, 1699.

17. Y. L. Lee, S. Kim, C. Park, J. Ihm and Y. W. Son, *ACS Nano,* 2010, **4**, 1345.

18. A. J. Du, Y. Chen, Z. H. Zhu, G. Q. Lu and S. C. Smith, *J. Am. Chem. Soc.,* 2009, **131**, 1682.

19. B. Huang, C. Si, H. Lee, L. Zhao, J. Wu, B.-L. Gu and W. Duan, *Appl. Phys. Lett.,* 2010, **97**, 043115.

20. A. J. Du, Y. Chen, G. Q. Lu and S. C. Smith, *Appl. Phys. Lett.,* 2008, **93**, 073102.

21. A. J. Du, Y. Chen, Z. H. Zhu, R. Amal, G. Q. Lu and S. C. Smith, *J. Am. Chem. Soc.,* 2009, **131**, 17 354.

22. O. Yazyev and L. Helm, *Phys. Rev. B,* 2007, **75**, 125408.

23. D. Boukhvalov, M. Katsnelson and A. Lichtenstein, *Phys. Rev. B,* 2008, **77**, 035427.

24. S. L. Lei, B. Li, E. J. Kan, J. Huang, Q. X. Li and J. L. Yang, *J. Appl. Phys.,* 2013, **113**, 213709.

25. P. Lou and J. Y. Lee, *J. Phys. Chem. C,* 2010, **114**, 10947.

26. Y. Cheng, Z. Zhu, W. Mi, Z. Guo and U. Schwingenschlögl, *Phys. Rev. B,* 2013, **87**, 100401.

27. Q. Chen, L. Y. Zhu and J. L. Wang, *Appl. Phys. Lett.,* 2009, **95** , 133116.

28. Y. D. Ma, Y. Dai, M. Guo, C. W. Niu, Y. T. Zhu and B. B. Huang, *ACS Nano,* 2012, **6**, 1695.

29. J. Mahmood, E. K. Lee, M. Jung, D. Shin, I.-Y. Jeon, S.-M. Jung, H.-J. Choi, J.-M. Seo, S.-Y. Bae, S.-D. Sohn, N. Park, J. H. Oh, H.-J. Shin and J.-B. Baek, *Nat. Commun.,* 2014, **6**, 6486.

30. G. Kress and J. Hafner, *Phys. Rev. B.,* 1993, **48**, 13115.

31. G. Kress and J. Furthmüller, *Comput. Mater. Sci.,* 1996, **6**, 15.

32. G. Kress and J. Furthmüller, *Phys. Rev. B.,* 1996, **54**, 11169.

33. J. P. Perdew, K. Burke and M. Ernzerhof, *Phys. Rev. Lett.,* 1996, **77**, 3865.

34. A. Kelly, A. M.-Castillo, L. Wang and T. E. Markland, *J. Chem. Phys.,* 2016, **144**, 184105.

35. B. M. Wong and J. G. Cordaro, *J. Phys. Chem. C,* 2011, **115**, 18333.

36. K. F. Mak, C. H. Lui, J. Shan and T. F. Heinz, *Phys. Rev. Lett.,* 2009, **102**, 256405.

37. D. M. Edwards and M. I. Katsnelson, *J. Phys.: Condens. Matter,* 2006, **18**, 7209.

38. E. C. Stoner, *Proc. R. Soc. London Ser. A,* 1939, **169**, 339.

39. J. F. Janak, *Phys. Rev. B,* 1977, **16**, 255.

40. G. Stollhoff, A. M. Oles and V. Heine, *Phys. Rev. B,* 1990, **41**, 7028.

41. P. Bruno and C. Chappert, *Phys. Rev. B,* 1992, **46**, 261.

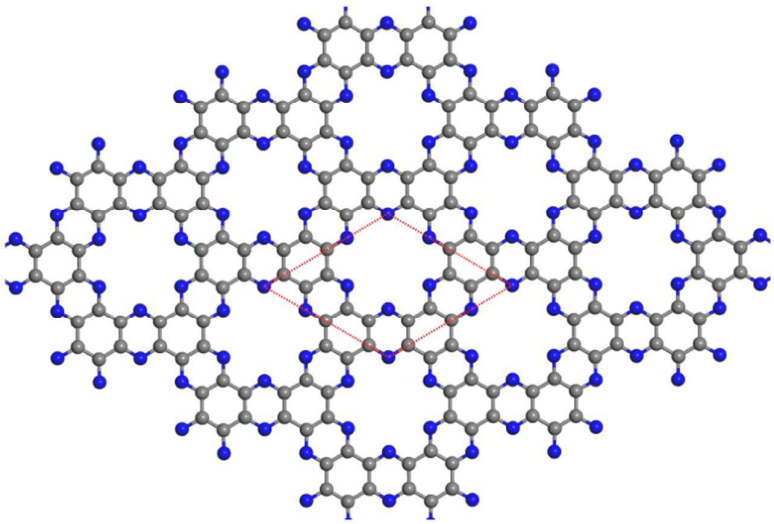

Fig .1. Top view of 2D *g*-C_2N. The dashed line shows a unit cell. Gray and blue balls represent C and N atoms, respectively.

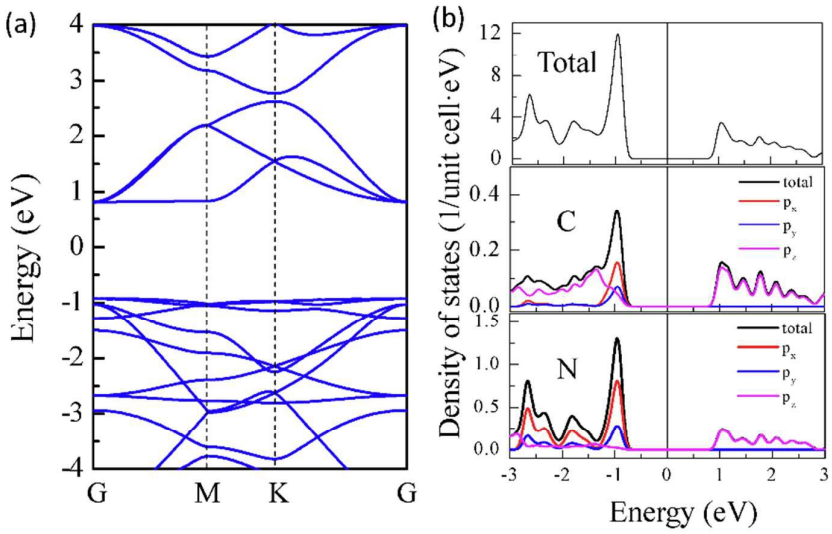

Fig. 2. Electronic structure of undoped 2D *g*-C_2N. (a) Band structure and (b) total DOS and partial DOS of 2D *g*-C_2N.

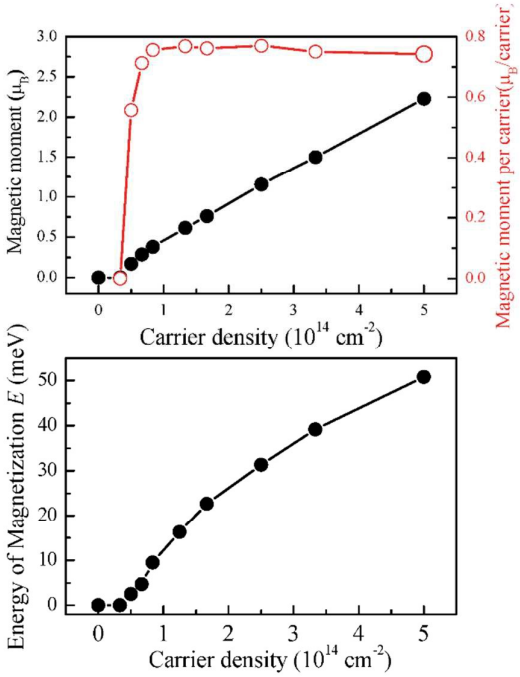

Fig .3. (a) Hole density dependent magnetic moment, magnetic moment /carrier and (b) the energy of magnetization.

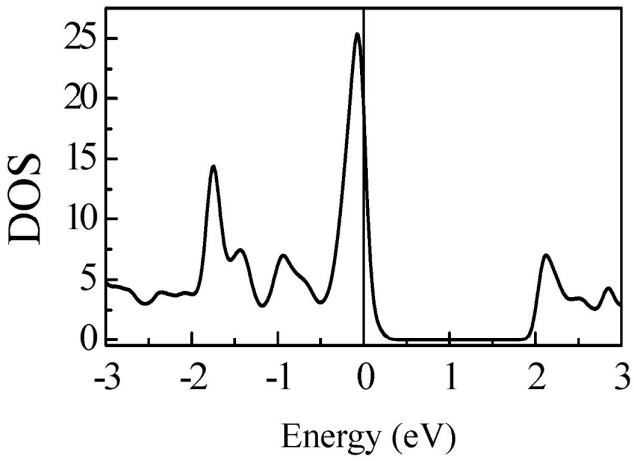

Fig. 4. The band structure of 2D *g*-C_2N at the doping concentration of 1.6×10^{14} cm^{-2} (1 hole per unit cell) without spin polarization.

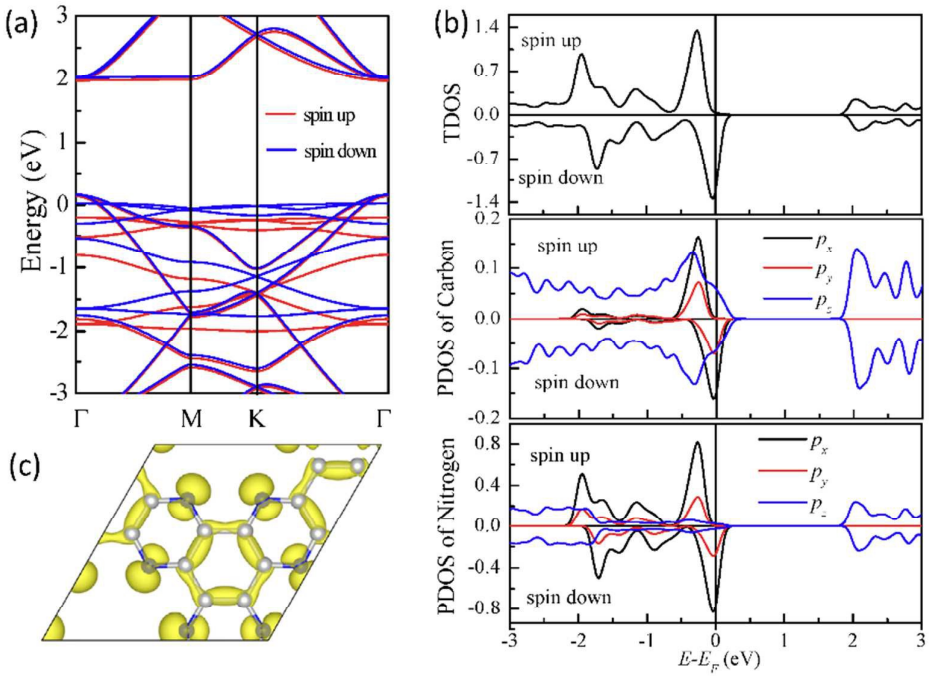

Fig. 5. Electronic structure of one hole doped 2D *g*-C_2N. (a) Band structure, (b) total DOS and partial DOS of 2D *g*-C_2N, and (c) spatial distribution of spin-polarized electron density.